A Single-Impulse System for Generating Solitary, Undulating Surge, and Gravity Shock Waves in the Laboratory

by

Robert L. Miller and Robert V. White

Technical Report No. 5

FLUID DYNAMICS AND SEDIMENT TRANSPORT LABORATORY
DEPARTMENT OF THE GEOPHYSICAL SCIENCES
THE UNIVERSITY OF CHICAGO
CHICAGO, ILLINOIS

June 1966

OFFICE OF NAVAL RESEARCH

Contract Nonr-2121(26)
NR 388-074

1. Introduction

Impulsively generated waves are of interest to the experimenter both from the point of view of laboratory analysis, and because of the several natural phenomena they represent, for example tsunami, and tidal bores.

The undulating surge-gravity shock wave forms have been generated in laboratory channels by means of the sudden release of an initial elevation above still water level. For example Prins, 1958, created the initial elevation by the partial evacuation of a plexiglass box placed in a tank. Sudden release of a sliding wall in the box created the desired waves. Wiegel, 1955, has studied impulsively generated two dimensional waves in a channel by creating a sudden movement of a submerged body, for a short interval of time. The system described in the present technical report could also be used very readily for the generation of solitary waves by using a combination of slower speeds and deeper initial water depth.

An alternative method for shock wave generation is suggested indirectly by Stoker 1957, who uses in his theoretical discussion of gravity shock waves, the physical analogue of a "piston" moving at constant velocity through a channel. He specifies for the case of interest here, " the 'piston' is accelerated instantaneously from rest to a constant forward velocity so that the piston curve is a straight line issuing from the origin in the x, t-plane." Although clearly the system to be described below does not accelerate instantaneously, the "rise time" from rest to constant velocity is quite short, and the wave generated during the run at constant velocity fits expectations rather well. The piston is stopped abruptly after travelling a fixed distance and a stable, repeatable, wave is produced. Several advantages over the vacuum-created initial

elevation method are noted.

1. It is possible to work on a rather large scale more practically than the vacuum-initial elevation method.

2. The very important parameter u (internal horizontal velocity component) can at least be estimated from the "piston" speed. In theoretical treatments plate or "piston" speed is considered to be equal to u.

2. The components of the system

The flow diagram fig. 2.1 indicates the components of the system used to drive the piston with the needed rapid acceleration to constant velocity, and the quick stopping characteristics.

The system is powered with a 3 phase A-C motor rated at 1.5 H.P. Shaft speed is controlled by a Graham variable speed transmission (Model 230 M), with input at 1750 r.p.m. and output at 0 to 1000 r.p.m. The output shaft is directly coupled to a Warner Electro-Pack magnetic clutch brake which is controlled by a spring loaded off-on switch. The switch leads into the clutch brake by means of a 50 foot extension cord so that the operator may conveniently position himself during an experiment. The magnetic clutch-brake allows for rapid coupling of the torque with the pulley-cable component, and provides a very efficient braking device. Details of the remote control, clutch brake system are given in figure 2.2.

The output shaft from the magnetic clutch brake is coupled directly to a Boston Reductor Ratio motor giving a 20:1 reduction in r.p.m. The output shaft transmits its torque to a pulley wheel mounted above by means of a chain link drive, as shown in fig. 2.3. The sprockets on the reductor and pulley shafts are of equal dimensions and tension is maintained in the chain drive by means of idlers. The grooved pulley wheels are 24 inches in diameter and lined with a special neoprene coating to minimize slippage. ¼ inch "airplane" cable is used because of its low stretching, strength, and resistance to rust and corrosion.

The "piston" is in the form of a 1" thick 12 3/4" by 4 ft. aluminum plate mounted on a wheeled cart as shown in fig. 2.4 . Rubber flanges extend the plate width to the full 14" channel width. The cart is a

permanent facility of the wave tank. The hard rubber-tired wheels ride on rails mounted on either side of the wave-tank. Order of magnitude calculations were made for carriage speed and force available in pounds of pull.

A. Maximum

1. Speed - Maximum output of the Graham is 1000 r.p.m. The 20:1 reductor yields an output of 50 r.p.m. Using a value of 2 feet for the pulley wheel, diameter, the towing speed is 5.2 feet per second.

2. Force - The rated output of the Graham is 125 inch-pounds at 1000 r.p.m. Output of the reductor gives a torque of 2500 inch lbs. Using a 2 ft. diameter pulley wheel as before, force = $\frac{\text{torque}}{\text{radius}}$, or approximately 208 lbs. of force available.

B. "Minimum"

1. Speed - A calculation was made for low speed near the anticipated minimum. At 100 r.p.m. the calculated speed is 0.52 feet per second.

2. Force - For the Graham, the noted torque at 100 r.p.m. is 45 inch-lbs. This yields 20 x 45 = 900 inch lbs. output from the Boston reductor.

$$\frac{\text{torque}}{\text{radius}} = \frac{900}{12} = 75 \text{ lbs of force available.}$$

For a still water depth of 0.5 ft., the following calculations were made of drag force to be expected over a piston speed range from 1 ft./sec to

6 ft./sec.

$$F_D = C_D \quad A \quad \frac{\rho V^2}{2}$$

ρ = 1.94 slugs/ft^3 at 60^{o}F

C_D = 1.16 for plate in which $\frac{x}{y} \cong 1$, from C_D vs R_e graph

A = 0.5 x 14 inches = 0.583 sq. ft. for immersed portion of piston.

V in ft/sec.	6	5	4	3	2	1
F_D in pounds	23.62	16.40	10.50	5.90	2.62	0.66

Allowing for inertia and friction of the system, in addition to the drag force of the piston, there is ample force available for the planned experiments.

3. Channel dimensions, slopes and roughnesses

The channel is formed by erecting a vertical partition of enameled 1 inch thick marine plywood in the wave tank facility. The partition parallels one of the glass sides of the tank, resulting in a channel 14 inches wide, 63 ft. long and 3 ft. deep with one wall glass through the full length. The slopes were erected inside the channel in the positions shown in fig. 3.1. The generating plate was run either left or right through the standard 8 foot run, depending on which slope was being used. The roughnesses k = .52 and 3.7 mm, were formed by coating the given slope with "double-sticky" tape Scotch brand, no. 4002Dcc V6724. Then glass beads of the desired size were sprinkled over the surface and pressed into place with a rubber coated roller. This process was continued until entire surface was close-packed with the glass spheres.

4. Calibration of Piston

The plate mounted on the wheeled cart, forms a piston system which for a given setting on the Graham control, will accelerate very rapidly to a constant velocity. The piston then moves along the channel at constant velocity pushing the fluid in front of it to form the desired wave characteristics.

Calibration of the actual piston speed in terms of the Graham motor control setting was carried out by means of strobe-flash photography. The glass walled side of the channel is marked into subdivisions of 1/10 foot throughout the length of stroke of the piston. The strobe-flash unit (Strobotac, type 1531-A) is a plug-in, operating on 60 cycle 110 volt power source. The flash originates from a strobotron lamp, activated by an electronic pulse generator. Flash rate ranges from 110 to 25,000 flashes per minute with an error of $\pm$ 1% of dial reading after calibration. The light intensity ranges from 0.6 million beam candles for high flash rate to 11 million beam candles for low flash rate.

Calibration of the flash rate is achieved with respect to the power line frequency, using screw driver control and neon indicator lamp system, which is supplied with the unit. Adjustment to error of less than $\frac{1}{2}$ of 1% is made without difficulty.

Through the range of Graham settings controlling the output shaft speed of the motor, the distance required by the piston to reach approximately constant velocity is dependent on magnitude of the constant velocity desired. Table 4:1 indicates that at nearly the highest plate velocity attainable with this system about 87% of the 8 foot run is at constant velocity.

Table 4:1

Distance required for plate to reach constant velocity from rest.

Constant velocity	Distance from rest	$\frac{\text{Accel. distance}}{\text{total run (8 ft.)}}$
.99 ft./sec.	.15 ft.	.0187
1.46 ft./sec.	.28 ft.	.0350
2.0 ft./sec.	.40 ft.	.0500
3.19 ft./sec.	.63 ft.	.0787
3.8 ft./sec.	.72 ft.	.0900
4.4 ft./sec.	.88 ft.	.1100
5.0 ft./sec.	1.00 ft.	.1250

Repeated images of the plate are recorded by an open-shutter Polaroid camera through the full 8 foot run. Good results were obtained with Polaroid 3000 speed/type 47 film. The flash rate was either 120, 240, or 480 per minute. In fig. 4.1 the successive plate images are ¼ sec. apart in time and approximately .36 ft. in distance, thus giving an average speed of 1.44 ft./sec. Interpolation between the 1/10 ft. lines was made with a template and magnifying glass. Note also that the distance between the successive images are very nearly equal, indicating that approximate constant velocity has been achieved, after the first 2 images. The image at the far right is the plate at rest. The plate is moving from right to left. Greater accuracy could be gained by refining the scale on the glass, and by increasing the strobe-flash rate. However it was considered that the degree of accuracy given here is sufficient for the purposes of the planned experiments.

Fig. 4.2 shows the line of best fit to the calibration data. The maximum deviation of data points from the fitted curve is 0.110 ft./sec and the average deviation is 0.026 ft./sec from the fitted curve. Over 300 individual runs were recorded.

5. Instrumentation for measurements

A. Wave gage recording system

The immediate purpose of this system is to provide the surface time history of the study wave as it passes the sensing element. See figs. 5.1, 5.2, 5.3. The gage is constructed of nichrome #30 wire, 6.28 ohms per foot resistance. The sensing wires operate on the basis of changing resistance; as the water level fluctuates, the pair of wires are shorted across, changing the resistive values. This results in a voltage change, which is compared to a constant voltage by use of a full-wave wheatstone bridge. See fig. 5.4. The basic design is patterned after the description given in Dean and Ursell, 1959.

The supply voltage to the bridge and wiring is a 5 volt 2400 c.p.s. signal. When the water in the wave tank is at rest, the bridge is balanced. In the balanced state, the voltage potential between arms a, b and c, d is zero. When motion occurs on the water surface causing resistance change in the sensing wires, the potential of arm a goes in either a positive or negative direction depending upon whether the water level rises or falls. This causes an unbalancing of the bridge.

The resultant voltage change from the bridge is transferred to a Sanborn Carrier Amplifier recorder, model 321. The 2400 C.P.S. carrier signal is demodulated and the voltage potential is fed into a millivolt recorder section. The changing signal activates a mechanical pen drive system which scribes a continuous line trace on mm. graph paper (fig. 5.5). A flow sheet, fig. 5.6, illustrates the interrelationships of the various components.

Calibration is achieved by a static method. The resistance probe sensing wires are raised and lowered by fixed increments in still water (usually 0.1 ft.) thus changing the water contact and hence the resistance in the wires.

The wave gage-resistance wire system is mounted on a Gurley point-gage with vernier as shown in fig. 5.7 so that accurate intervals may be obtained during the raising or lowering process.

B. Celerity (wave velocity) measurements.

The measurement of wave celerity for the undulating surge-shock wave types proved to be difficult. In the undulating surge range the smooth crests were rather flat except near the transition range, and thus it is difficult to determine a repeatable datum point for use during replicate runs of the same wave. In the shock wave range the extreme turbulence of the wave front causes wide fluctuations in local celerity. Furthermore the violent eddy motion creates a variable wave profile in the front portion so that once again it is very difficult to find a repeatable datum point for replicate runs of the same wave. Three methods were devised to meet these difficulties.

1) Contact probes

The scheme used in this case, is to take the average wave celerity over a distance along the path of travel, significantly larger than any length involved in the local motions of the wave front. In terms of the physical dimensions of the waves generated in the test channel, a distance of 1 foot was chosen. Due to surface tension in the water, an upcurving of the water surface in front of the oncoming wave was noted, leading smoothly into the wave front proper. This upcurving is utilized for several purposes and will be referred to again. It is illustrated in photograph of fig. 6.1, and is also recorded in the Sanborn oscillograph records, see fig. 5.10. In the present instance, two electrical contact probes are placed 1 foot apart along the midline of the channel. The contact points are adjusted so that they are just clearing undisturbed water surface.

Thus, as the wave progresses down channel, the initial upcurving of the water surface which just precedes the wave front, contacts the point of the first probe. This is recorded in the first channel of a Sanborn oscillograph.

The same signal is recorded as the second probe located 1 foot down-tank is contacted by the rise in water level. The chart drive of the Sanborn oscillograph is utilized as a timer with chart speed usually set at 100 mm/sec. Thus, the distance between analogous signals on the two channels of the Sanborn in mm, is a measure of travel time of the wave over the 1 foot standard distance.

The contact probe is actually the Gurley point gage, in which a current is passed into the pointed rod portion of the gage, see fig. 5.8 which acts as a simple lead. The tank itself (through the water) is connected to the grounded side of a 50 trim-pot, and a wheatstone bridge is utilized as shown in fig. 5.9. Each probe is connected to the "high side" of the 50Ω trimpot, which forms part of arm A of the bridge.

The method is effective but crude. Clearly, utilizing the chart drive speed of the Sanborn oscillograph as a timer leads to inaccuracy. At 100 mm./sec chart speed, tests with a 10 sec per full revolution stop watch indicated a maximum error of ±5mm per second, e.g. ±5% error. Further difficulty lies in the fact that the upcurve of the water surface in front of the oncoming wave varied in degree of curvature, particularly in comparison between an undulating surge and a well developed shock form. This introduces error not among replicates of the same wave, but between the various waves through the full Froude number range.

2) Comparison of oscillograph records from two wave gages.

In this case the same general technique is utilized as in the case of the contact probes. In place of two contact probes placed 1 foot apart along the channel midline, two wave gages are used. A datum point is chosen on a given wave from the oscillograph trace, for example, as the crest of the leading undulation in an undulating surge wave. The distance between this point and the same datum point on the second wave record taken 1 foot down stream is converted to time. This yields an estimate of average wave celerity. This method proved to be the least satisfactory. It suffers not only from the inherent time error due to chart speed fluctuation, but also from considerable subjectivity in choosing a datum point which bears the same relation to the wave in the first recording as in the second. This difficulty is most marked in the shock-range.

3) Motion picture camera.

The most satisfactory technique used involves the use of a motion picture camera. The camera is a 16mm Bolex H 16 Reflex, equipped with a Switar f=10mm wide-angle lens. At a distance of 3.5 feet the field is about 3.3 ft. square. The glass walled test section is scribed in units of 1/20 foot in both horizontal and vertical. Camera speed is set at 64 frames/sec. An electric timer (Standard Electric, Model S-1) 1 second full revolution, with 1/100 second subdivisions, is placed against the glass walled test section so that it appears in the upper corner of the field without obscuring full view of the wave. The camera is placed so that it photographs the wave profile, and is focused on the inner side of the glass wall. Satisfactory photographic results were obtained with Kodachrome II Photoflood film. The water was colored with Rhodamine B (Allied Chemical) dye which gave a desirable contrast of the water against the white inner wall of the channel.

Careful comparison of the electric timer with frame speed indicated that frame speed at 64 frames/sec varied less than one half of a percent. The developed film is placed in a Craig Projecto-editor film viewer and the forward progress of the wave is measured against the grid on the glass wall, 1 frame at a time (e.g. 1/64 second) per frame. For some purposes it would be quite feasible to approach $\frac{dx}{dt}$ by using the additional aid of strobe flash lighting. However in the present case $\frac{\Delta y}{\Delta t}$ is measured with Δt at 1/16 sec. Thus we read the wave front advance every four frames on the on the viewer. The fluctuations in forward progress per unit t (1/16 sec.) are indicated in figs. 6.4,6.5 in section 6 .

Choice of datum point in the undulating surge range is the crest of the leading undulation. In the low Froude number wave the crests are rather flat as referred to earlier. However the grid on the glass wall facilitated a standard order of procedure e.g. to consider the portion of the crest which crosses the highest horizontal grid line as an arc, and take the midpoint of the corresponding chord along the highest horizontal grid line as the crest.

Lighting of the test section was done by arrangement of a number of flood lamps. An "edge-lighting" effect was achieved on the water surface by using a low angle flood lamp. The result is a bright line which reproduces the water surface in profile almost graphically in the developed film. The datum point in the shock form was designated to be that point just in front of the wave where the bright line abruptly ends due to the turbulent wave front.

C. Oscillograph records and still photographs of the undulating surge and gravity shock waves.

When a wave is propogated down-channel, the signal from the resistance wave gage described earlier in this section, is recorded on a Sanborn oscillograph. With proper calibration and assuming the effect of non-linearity is small enough to be neglected, the resistance wave gage-Sanborn oscillograph system will give reliable measurements of the wave height in the undulating surge range. However, the horizontal-dimension of the wave trace is a function of paper speed, so that a complete picture of the geometry of the wave requires other methods. For this purpose optical measurements were utilized.

The form and dimensions of the plate-generated wave as it travels over the flat section of the channel, is illustrated by Sanborn oscillograph record and corresponding photographs of fig. 5.10a, b,c,d.

The still photographs were taken with a Polaroid 110B camera using 3000 no. 47 film. Measurements of y_2 (the wave height) were found to be about equally reliable from oscillograph or film in the undulating surge range. However, in the highly turbulent shock range with the expanded aerated wave front, the photos were much more reliable for selection of the flat portion behind the wave front, from which y_2 is measured.

6. Comparison of basic gravity shock wave characteristics expected from theoretical considerations, with the experimental shock wave characteristics.

The purpose of the present study is to establish experimentally certain characteristics of gravity shock waves. It is therefore necessary to establish the degree to which the basic characteristics of the initial gravity shock wave created in the laboratory channel, agrees with the theoretical expectations.

Consider an open channel with a non-sloping bottom. The channel is filled with water to a depth y_1, and a piston is located at one end with plate width corresponding to the width of the channel. The piston is brought rapidly from rest to constant velocity. It continues down channel for a short distance[1], then is abruptly brought to rest, releasing the wave for study. Fig. 6.1 shows a sequence of photographs of the initiation early phases and full development of the stable shock wave, as well as the coupling of the plate with the water.

The plate moves from left to right in the diagram with velocity V. At a given instant in time, the fluid volume displaced is V dt y_2, where y_2 is the distance from channel bottom to the created water level as indicated in figure 6.2. We will consider the channel to be unit width in what follows. The resulting advance of the wave front with velocity C must increase the volume of the disturbed fluid by a corresponding amount. By continuity, the two volumes (crosshatched in the figure) must be equal. Equating these volumes and cancelling dt on both sides,

---

[1]The stroke length of the piston at constant velocity has considerable effect on the run-up. Therefore in all run up experiments the travel characteristics of the piston are held to a fixed standard. The plate starts from rest, travels 8 ft. and then stops abruptly. The wave travels an additional 4 feet over the flat bottom, then begins to climb the study slope.

$$C \cancel{dt} (y_2 - y_1) = V \cancel{dt}\, y_2 \qquad \text{eqn. 1}$$

which is the continuity expression for this case.

We now equate the resultant force to the rate of momentum change. The fluid volume y_1 C dt acquires momentum ρ V of the disturbance. The rate of momentum change is $\frac{d \rho V}{dt}$. The full expression is then y_1 C dt $\frac{\rho\, dV}{dt}$, or y_1 Cρ dV. The resultant force is taken to be the difference in hydrostatic pressure over normal sections on either side of the wave front, illustrated in fig. 6.2 .

$$\gamma \int_0^{y_2} y\, z\, dy - \gamma \int_0^{y_1} y\, z\, dy$$ = difference in hydrostatic pressure on either side of the wave front.

where γ is the specific weight of the fluid, and the channel width ~~z~~ is taken to be unity. Carrying out the integration yields the term.

$$\frac{\gamma}{2} (y_2^2 - y_1^2)$$

Now, equating resultant force to rate of momentum change,

$$\frac{\gamma}{2} (y_2^2 - y_1^2) = y_1 C \rho\, dV \qquad \text{eqn. 2}$$

According to Stoker, (1957) the gravity shock wave must satisfy equations 1 and 2 above. The relations given in equation 1 and 2 may be conveniently compared with the observed data in terms of the parameter $\frac{y_2}{y_1}$. The wave height (measured from the bottom as y_2) is the most and accurately easily measured characteristic of the wave.

1) Plate velocity V vs. y_2/y_1.

The plate velocity V is also considered to be equivalent of the horizontal velocity u of the fluid particle under the wave.

We have, $C = \frac{V\, y_2}{y_2 - y_1}$ from equation of continuity, eqn.1.

substituting in eqn. 2 and rearranging terms,

$$\left(\frac{\gamma}{2}\right) y_2^3 - \left(\frac{\gamma}{2} y_1\right) y_2^2 - \left(\frac{\gamma}{2} y_1^2 + y_1 \rho V^2\right) y_2 + \left(\frac{\gamma}{2} y_1^3\right) = 0$$

which is a cubic in y_2. This may be written after dividing through by

$\gamma/2$ and by y_1^3 as

$$\left(\frac{y_2}{y_1}\right)^3 - \left(\frac{y_2}{y_1}\right)^2 - \left(1 + \frac{2\rho V^2}{g y_1}\right)\frac{y_2}{y_1} + 1 = 0$$

let $\frac{y_2}{y_1} \equiv r$, and $\sqrt{\frac{g y_1}{\rho}} = \sqrt{g y_1} = C_1$,solving for V

$$V^2 = \frac{C_1^2}{2r}(r^3 - r^2 - r + 1)$$

or $$\frac{V}{\sqrt{g y_1}} = \left(\frac{y_2}{y_1} - 1\right)\sqrt{\frac{y_2/y_1 + 1}{2\, y_2/y_1}} \qquad \text{eqn. 3}$$

Figure 6.3 shows a plot of the dimensionless parameters $\frac{V}{\sqrt{g y_1}}$ vs. $\frac{y_2}{y_1}$ where the experimental points are compared with the curve calculated from eqn. 3.

The fit is quite close although consistently higher than the calculated curve for $y_2/y_1 > 1.5$, and consistently lower than the curve for $y_2/y_1 < 1.5$.

2) Wave velocity C, vs, y_2/y_1

Substitution of the continuity eqn. in eqn. 2 yields an expression for wave celerity C, as a function of g, y_1 and y_2

$$C = \sqrt{g y_1}\left[\frac{1}{2}\, y_2/y_1 \left(y_2/y_1 + 1\right)\right]^{1/2} \qquad \text{eqn.4}$$

Experimental data is compared with the calculated curve in dimensionless form, $\frac{c}{\sqrt{gy_1}}$ vs, $\frac{y_2}{y_1}$ in fig. 6.4 where c is the experimentally observed value of C. As in the previous graph the observed data falls below the calculated curve for $\frac{y_2}{y_1} < 1.25$. For $y_2/y_1 > 1.25$, the trend of the data follows the curve, although widely scattered. The scatter increases markedly at $\frac{y_2}{y_1} > 2.0$ and in the higher ranges, the scatter is extreme. Fig. 6.5 gives a comparison of deviation in local celerity from the theoretical expectation, for shock range vs undulating surge plus transition range. Considerable difficulty was encountered in measuring the celerity, particularly above the transition from undulating surge to shock form. The difficulty was due in part to the extreme turbulence of the wave front, and in part to the aeration of the wave front. The data given in fig. 6.4 was obtained by using motion picture photography and represents the best results in comparison with two other techniques using electrical signals. Details are given in section 5, on measurements.

7. Conclusions and Summary.

The system appears to work satisfactorily for experimental studies. It is flexible in output and yet generates a given wave with quite close repeatability. Comparison of observed with expected values for V vs y_2 and C vs y_2 seem to fit as close as could be expected if one takes into account the effects of wall and bottom roughness, and the strong aeration during the progression of the shock wave form.

NOTATION

c	Celerity (experimentally observed wave velocity)
k	Roughness diameter
r	y_2/y_1
r.p.m.	revolutions per minute
t	time
u	horizontal component of water particle velocity
x	horizontal coordinate axis, along the wave channel length
y	vertical coordinate axis, measured positively upward, zero at channel bottom
y_1	undisturbed water depth, measured up from channel bottom
y_2	wave height, measured up from channel bottom
A	cross section area
C	celerity (theoretical expectation of wave velocity)
C_D	coefficient of drag
C.P.S.	cycles per second
F_D	drag force
Re	Reynolds number
V	piston velocity
z	horizontal coordinate axis across channel width
γ	specific weight, $\frac{Mg}{\text{Unit volume}}$
Ω	ohm, the unit of electrical resistance
ρ	density

REFERENCES

Dean, R. G. and Ursell, F., 1959, Interaction of a Fixed Semi-immersed Circular Cylinder with a Train of Surface Waves. Mass. Inst. Technol. Tech. Report No. 37, Hydrodynamics Lab. M.I.T., Cambridge, Mass. 91 pp.

Prins, J. E.,1958, Characteristics of Waves Generated by a Local Disturbance, Trans. Amer. Geophys. Union.39, 5 pp. 865-874.

Stoker, J. J., 1957, Water Waves. The Mathematical Theory With Application. Interscience Publishers Inc. N. Y. 567 pp.

Wiegel, R. L,, 1955, Laboratory Studies of Gravity Waves Generated by the Movement of a Submerged Body. Trans. Amer. Geophys. Union., 36,5 pp. 759-774.

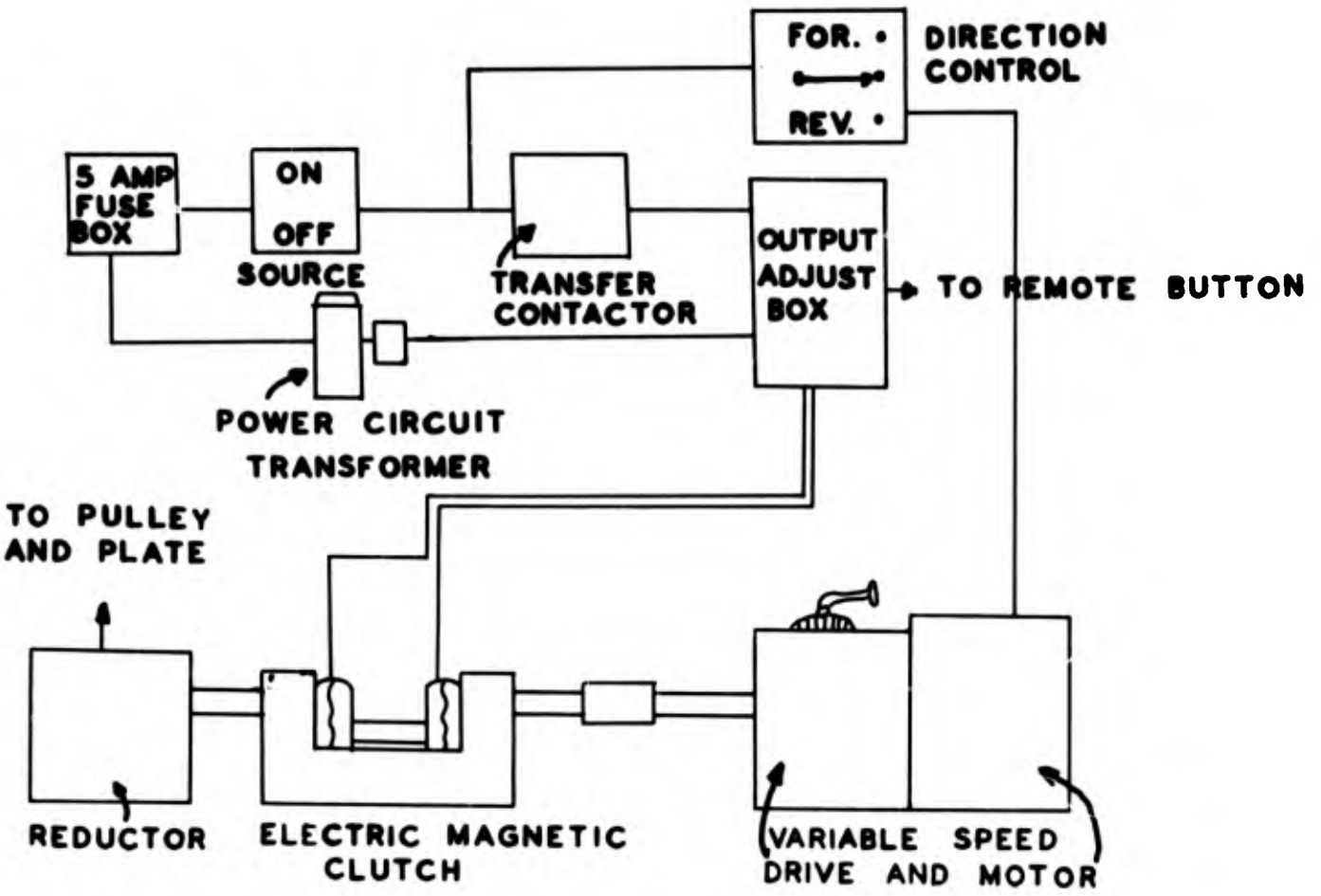

BLOCK DIAGRAM OF SHOCK PLATE CONTROL SYSTEM

Figure 2.1

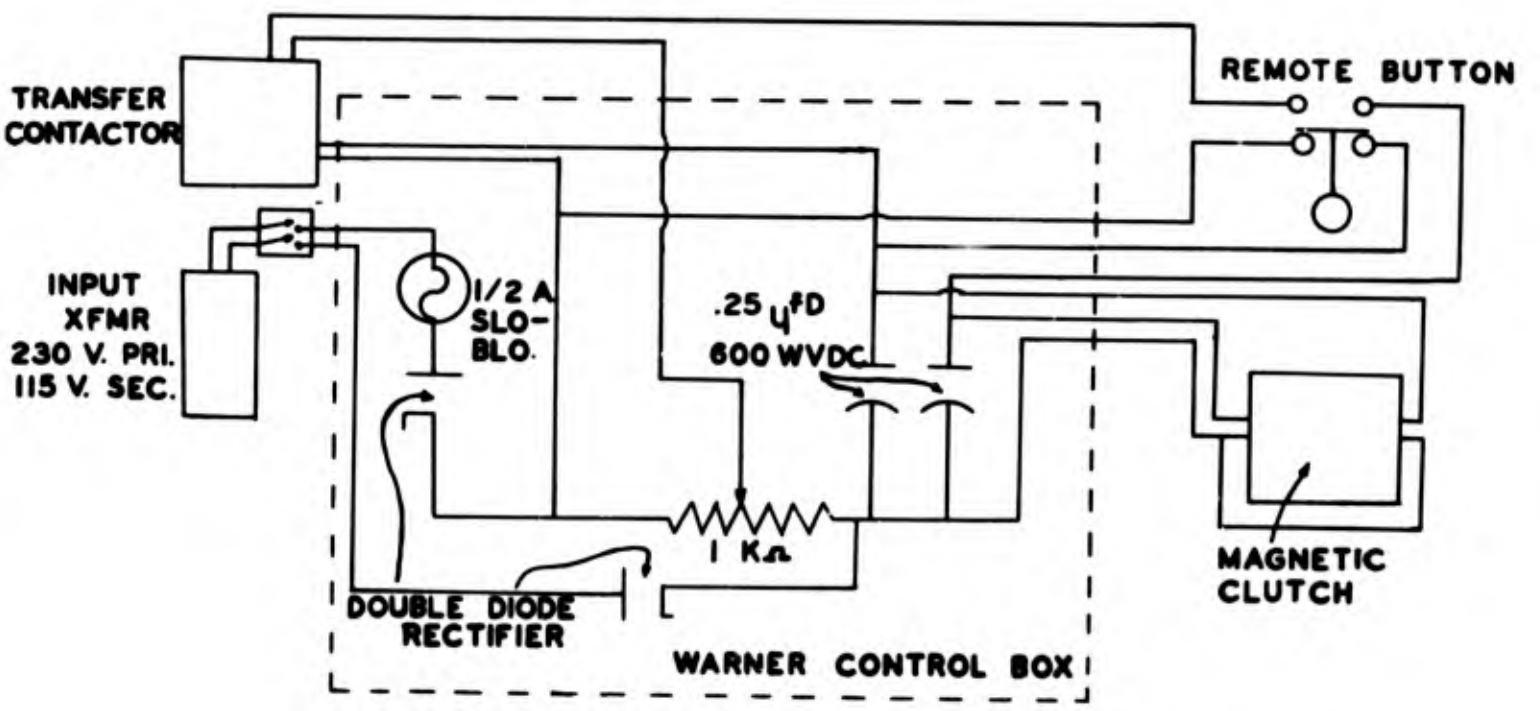

SCHEMATIC OF WARNER CONTROL BOX, REMOTE CONTROL BUTTON, AND EXTERNAL CONNECTIONS.

Figure 2. 2

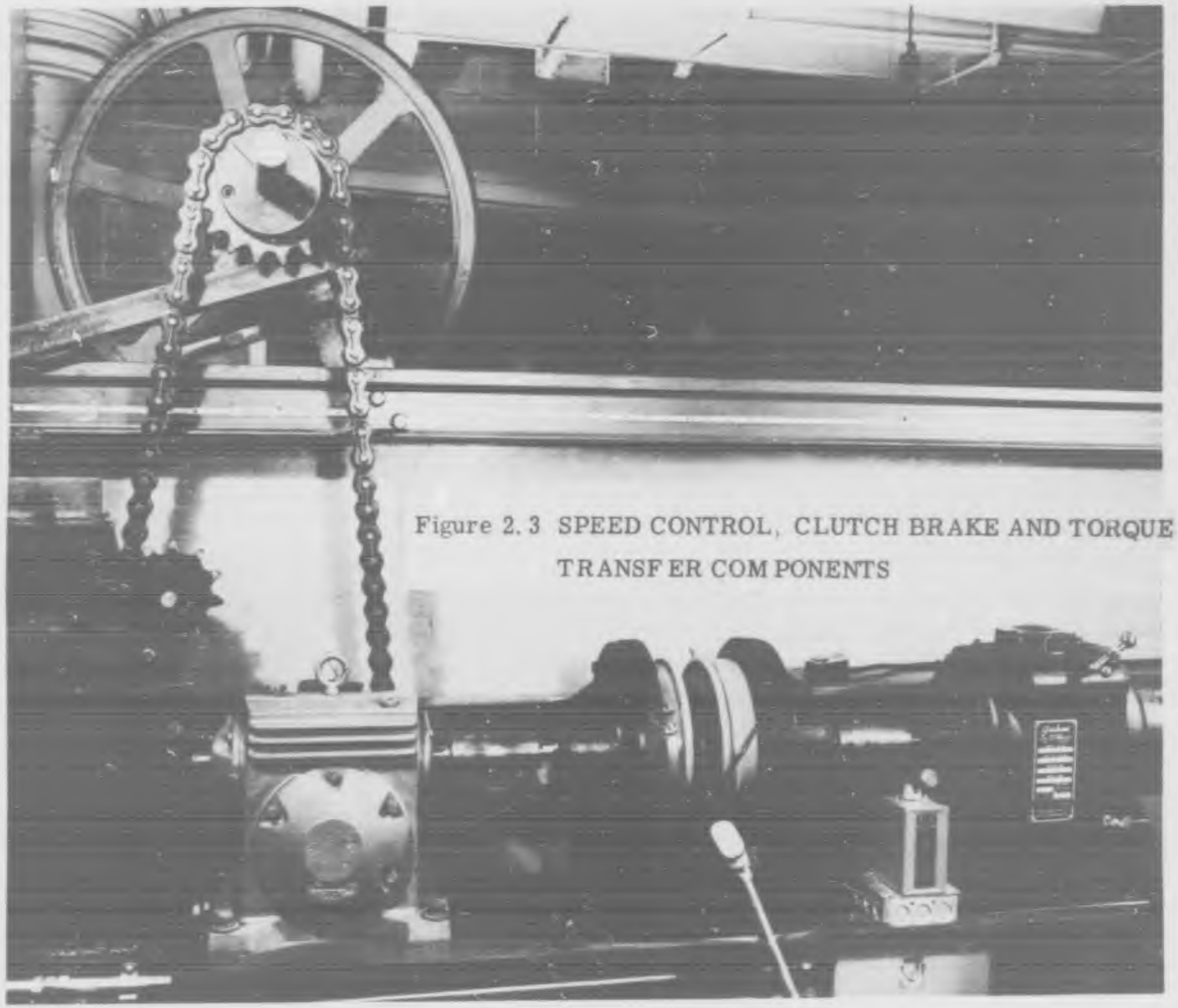

Figure 2.3 SPEED CONTROL, CLUTCH BRAKE AND TORQUE TRANSFER COMPONENTS

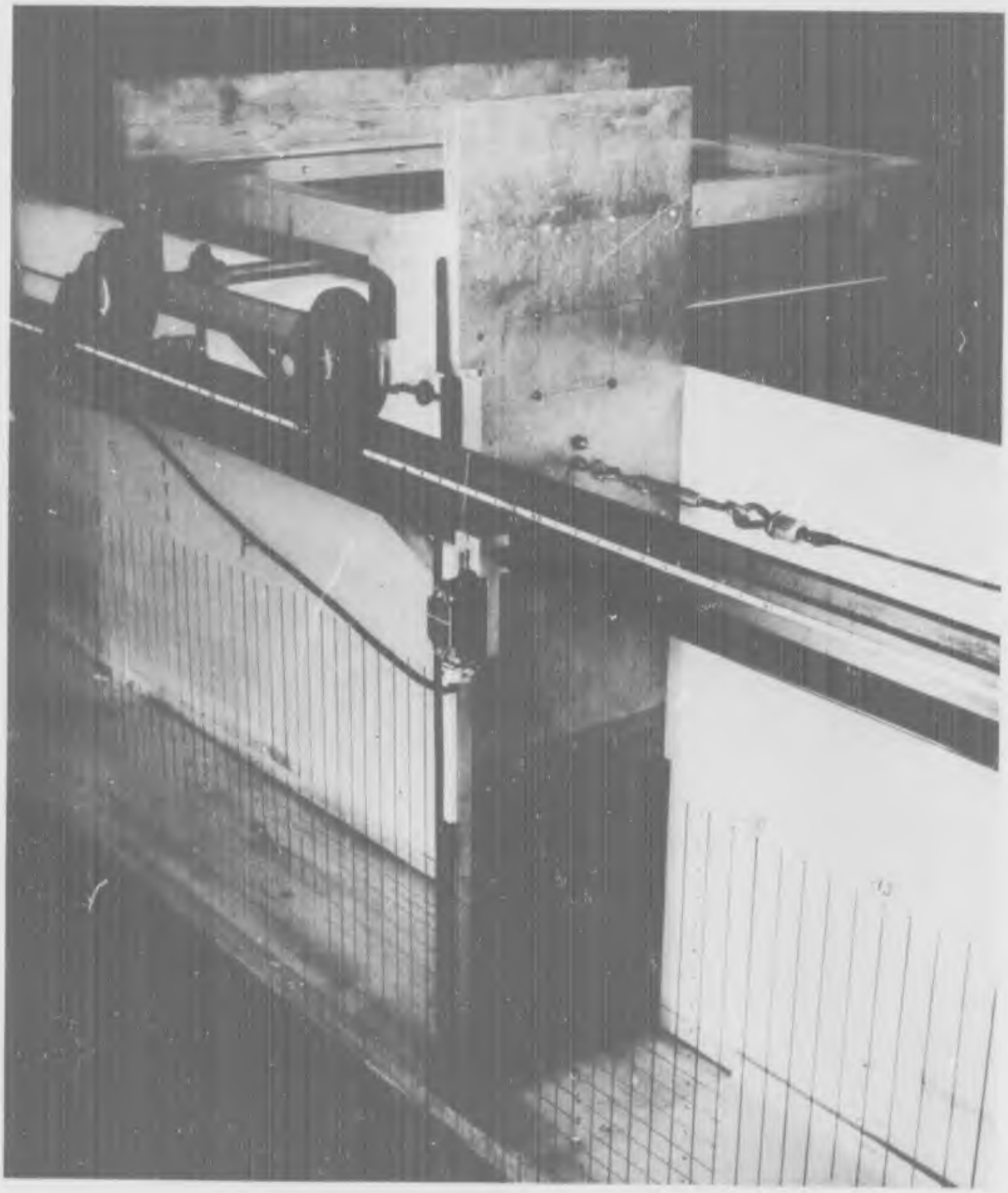

Figure 2.4 PISTON AND WHEELED CART

Figure 3.1 SCHEMATIC OF CHANNEL DIMENSIONS AND TEST SLOPES

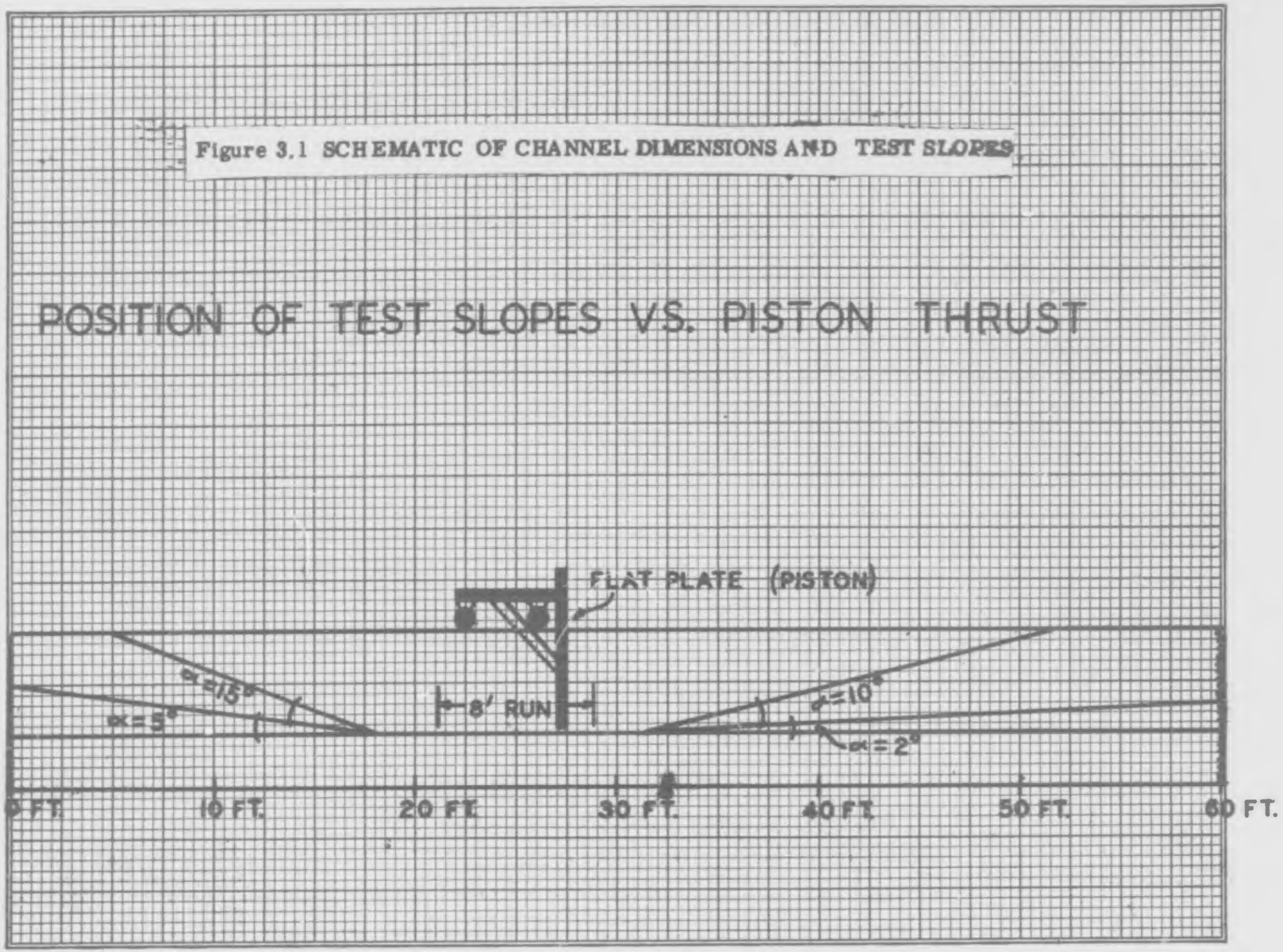

Figure 4.1

STROBE FLASH PHOTO SHOWING

PISTON ACCELERATING FROM REST TO CONSTANT VELOCITY

Figure 4.2

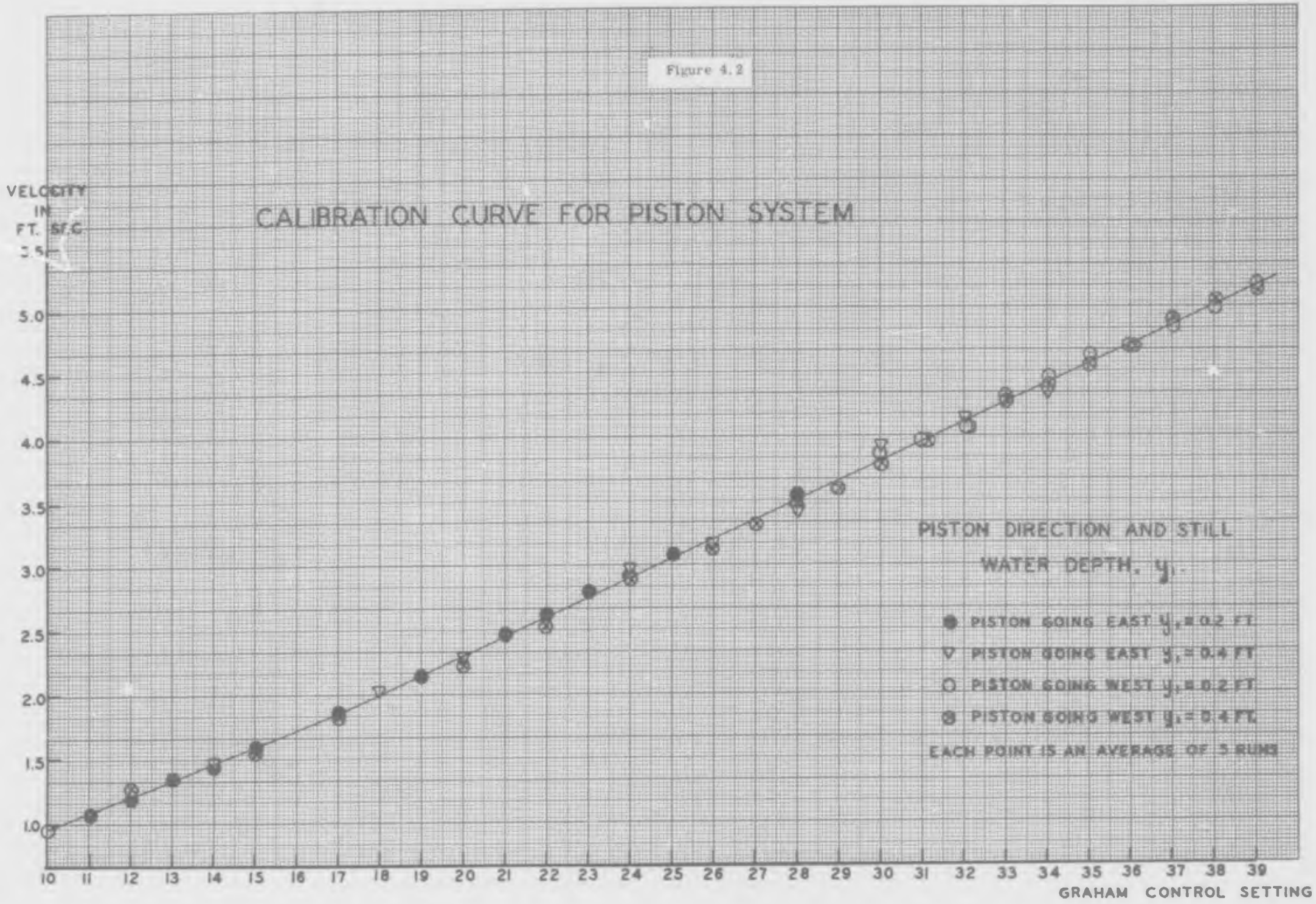
CALIBRATION CURVE FOR PISTON SYSTEM
VELOCITY IN FT. SEC.
5.5
5.0
4.5
4.0
3.5
3.0
2.5
2.0
1.5
1.0
10 11 12 13 14 15 16 17 18 19 20 21 22 23 24 25 26 27 28 29 30 31 32 33 34 35 36 37 38 39
GRAHAM CONTROL SETTING
PISTON DIRECTION AND STILL WATER DEPTH, y_1.
PISTON GOING EAST y_1 = 0.2 FT
PISTON GOING EAST y_1 = 0.4 FT
PISTON GOING WEST y_1 = 0.2 FT
PISTON GOING WEST y_1 = 0.4 FT
EACH POINT IS AN AVERAGE OF 5 RUNS

Figure 5.1 RESISTANCE WIRE PORTION OF WAVE GAGE SYSTEM
(Two gages are shown in position in the wave channel)

Figure 5.2

RESISTANCE TYPE WAVE GAGE
SIDE VIEW

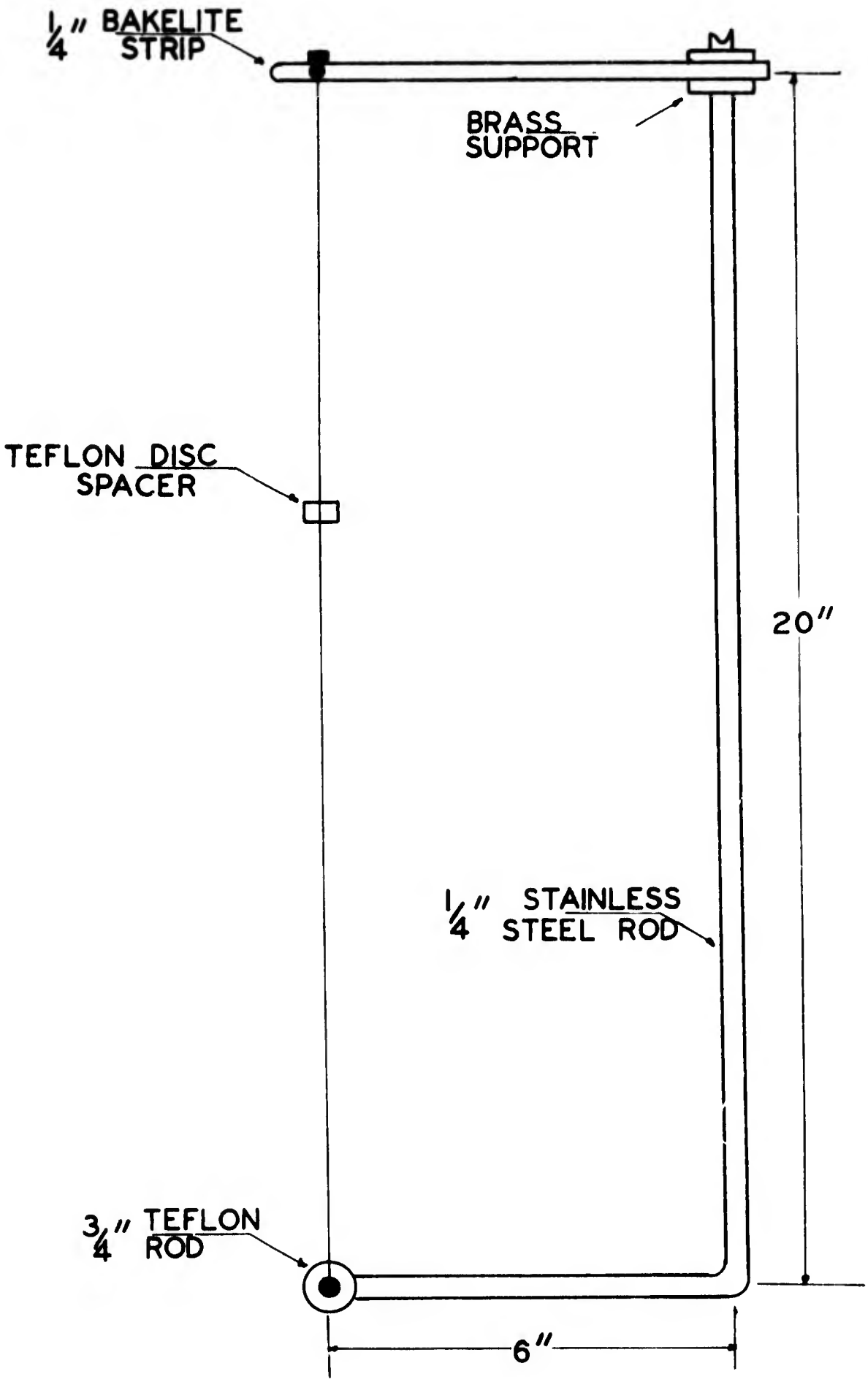

Figure 5.3

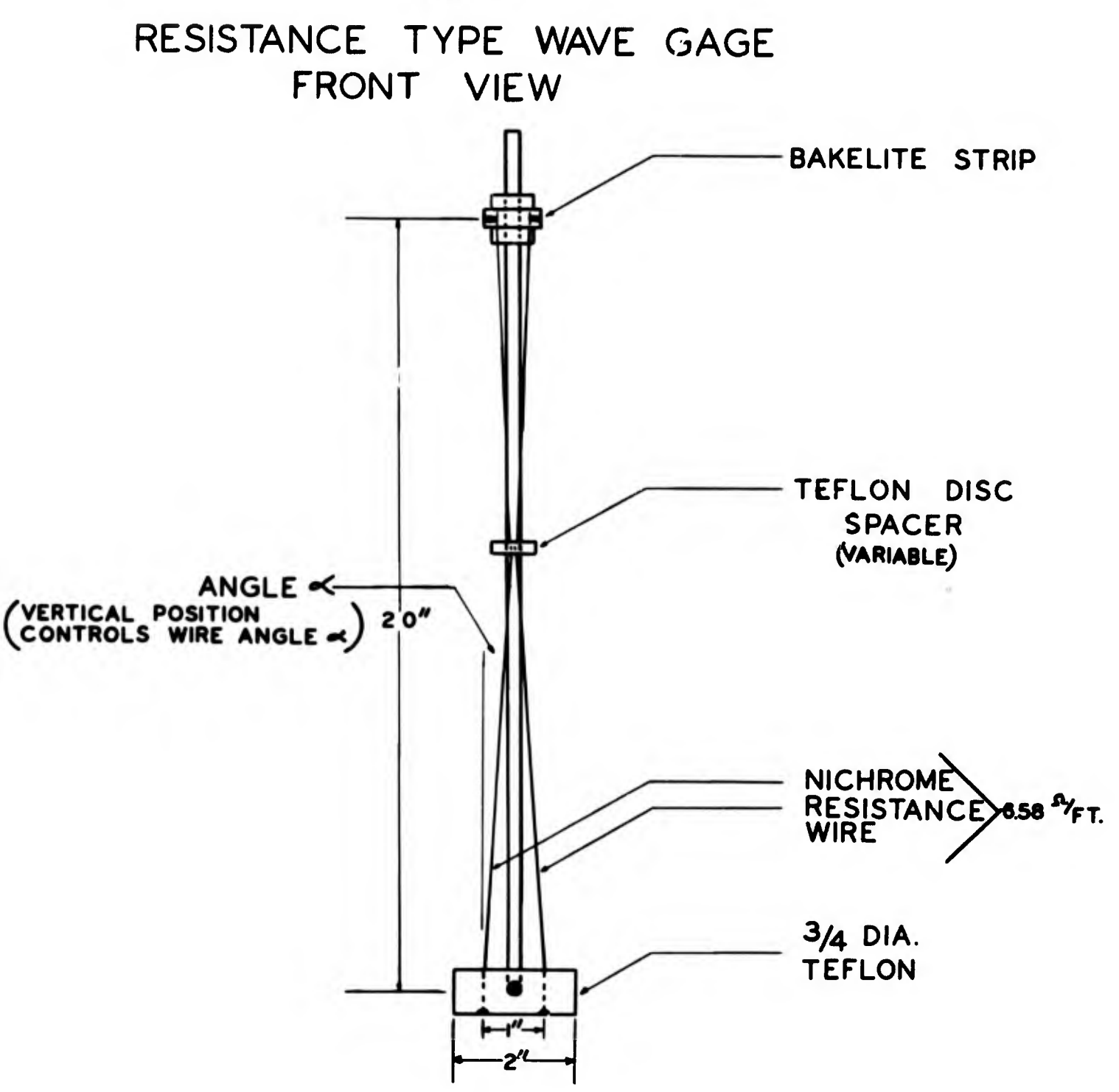
RESISTANCE TYPE WAVE GAGE
FRONT VIEW
BAKELITE STRIP
TEFLON DISC
SPACER
(VARIABLE)
ANGLE
(VERTICAL POSITION
CONTROLS WIRE ANGLE)
20"
NICHROME
RESISTANCE
WIRE
6.58 Ω/FT.
3/4 DIA.
TEFLON
1"
2"

Figure 5.4

FULL WAVE WHEATSTONE BRIDGE WITH RESISTANCE WAVE GAGE CONNECTIONS

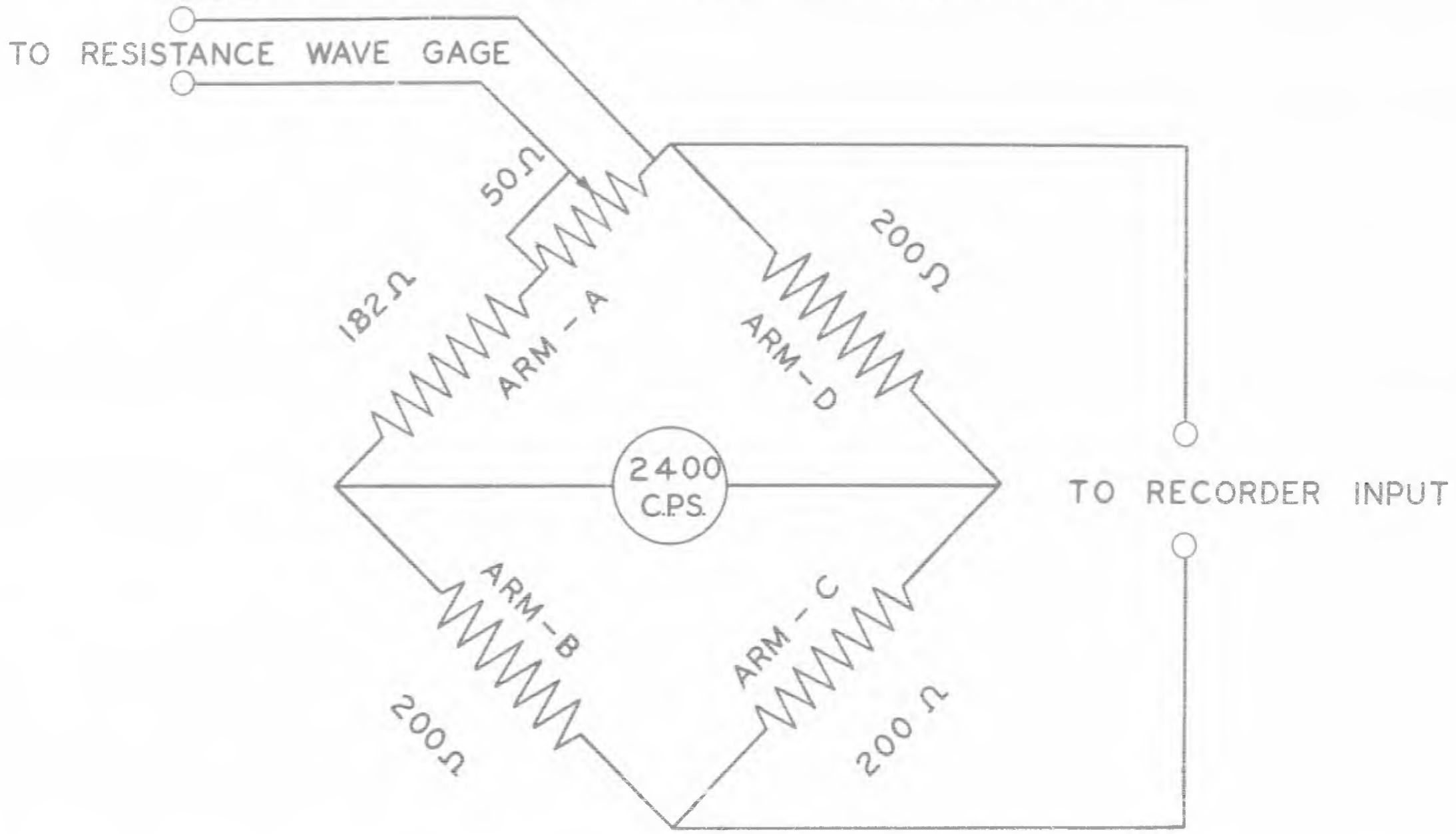

Figure 5.5

OSCILLOGRAPH RECORD OF WAVE TRACE FROM TWO GAGES

(A single wave is recorded twice, the signal on the right is 1 foot further down channel than the signal on the left.)

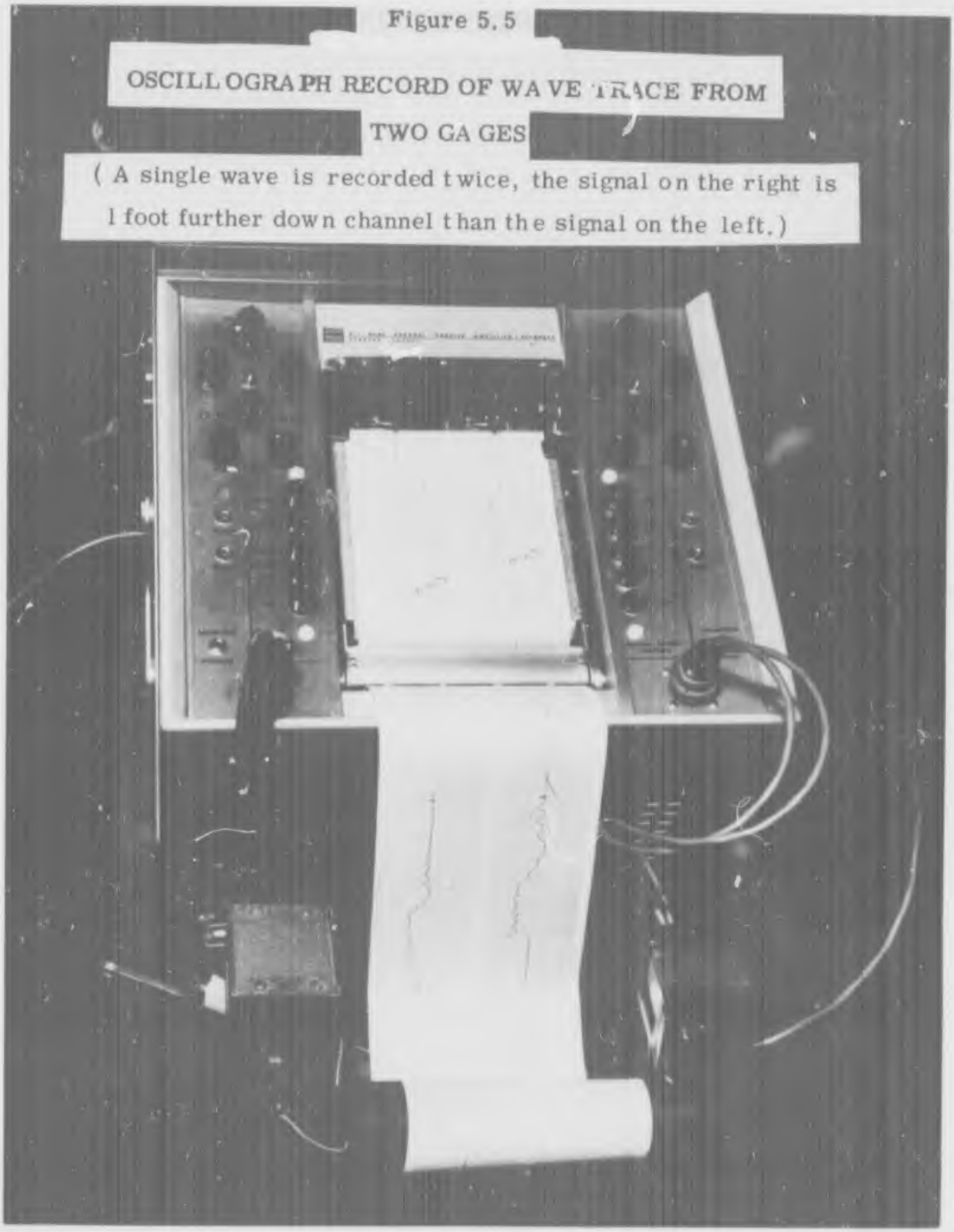

Figure 5.6

BLOCK DIAGRAM OF WAVE RECORDING SYSTEM

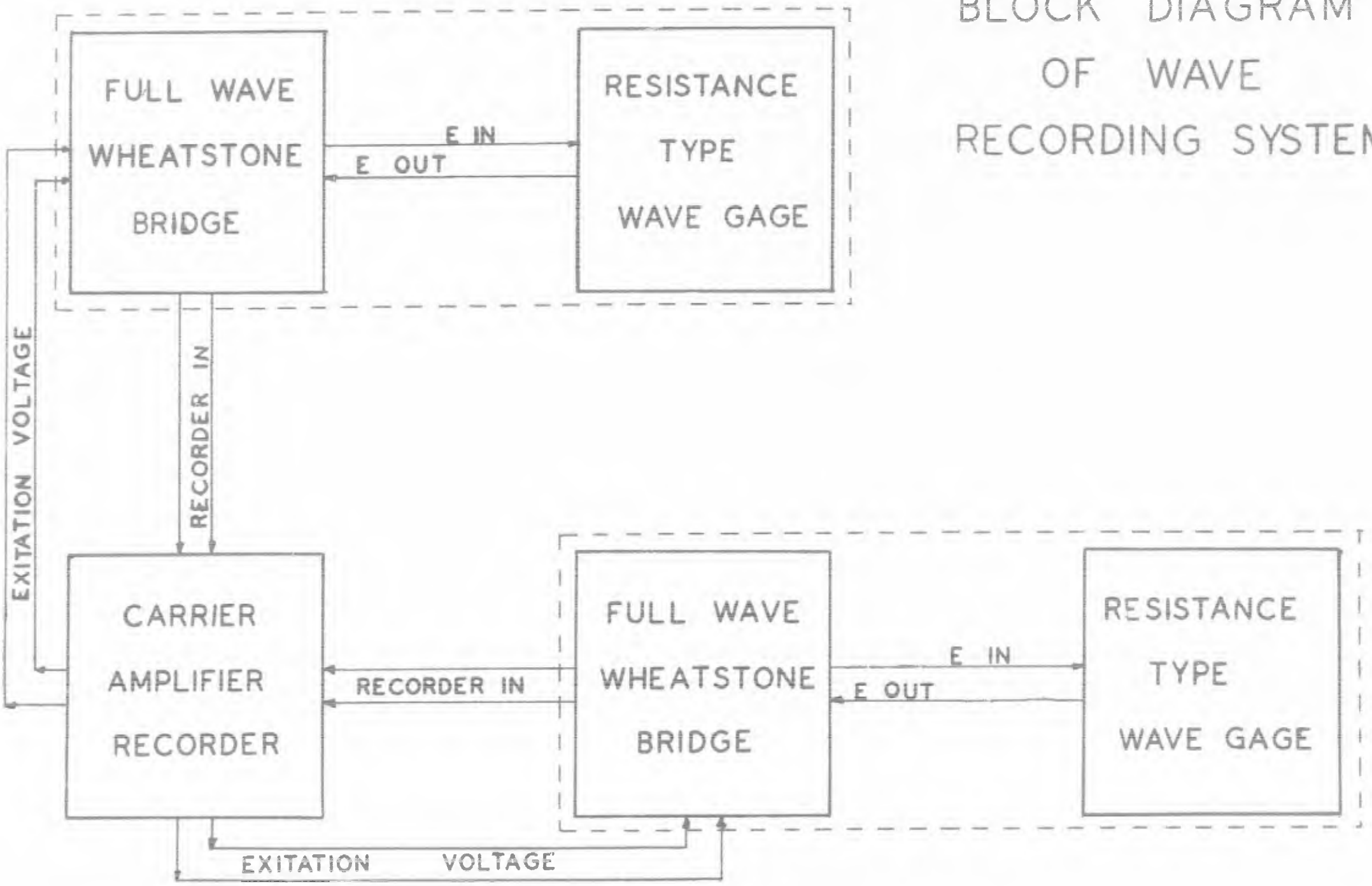

Figure 5.7 CALIBRATION MOUNTS FOR RESISTANCE WIRES

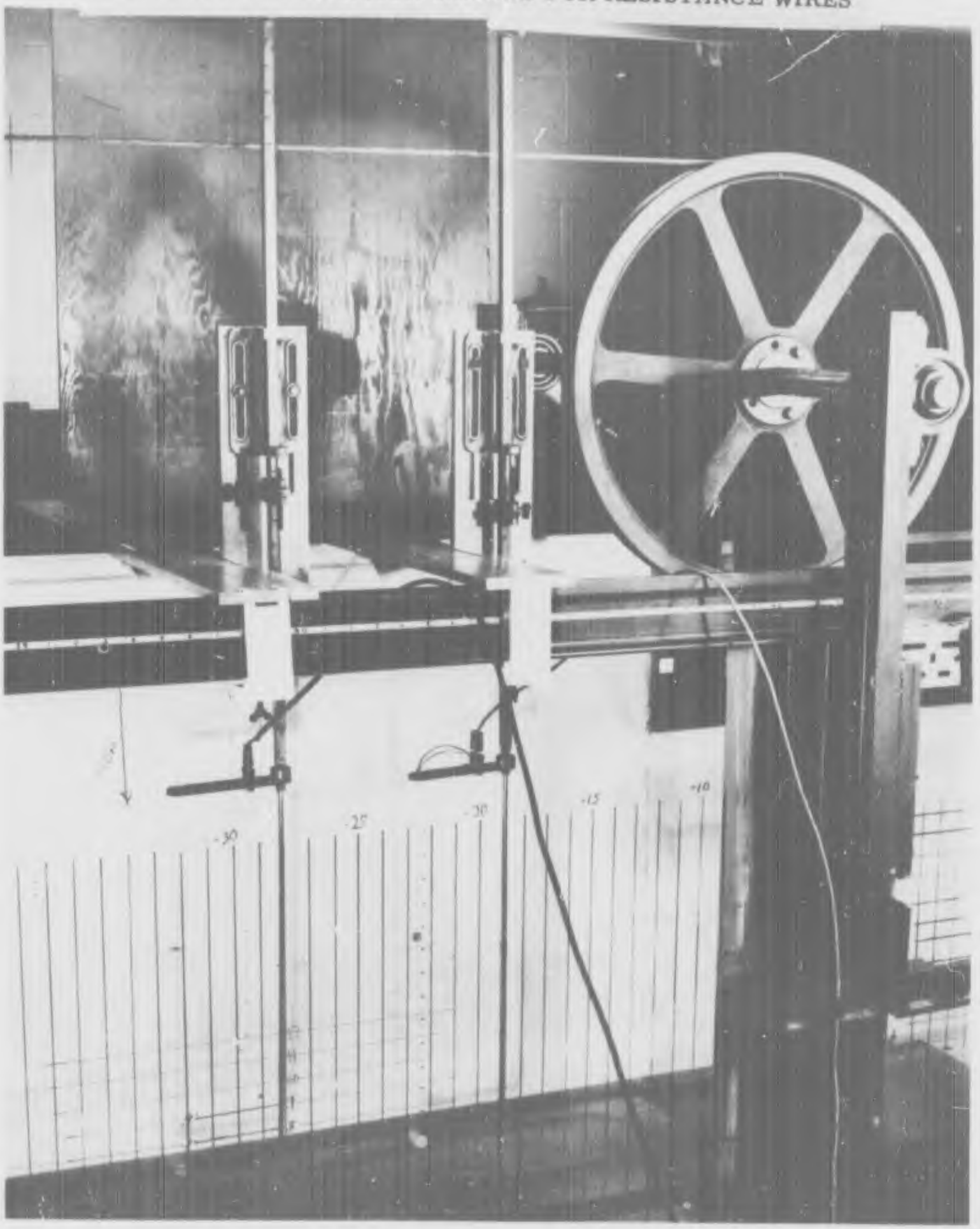

Figure 5.8

POINT GAGES MODIFIED AS SIMPLE ELECTRICAL LEADS

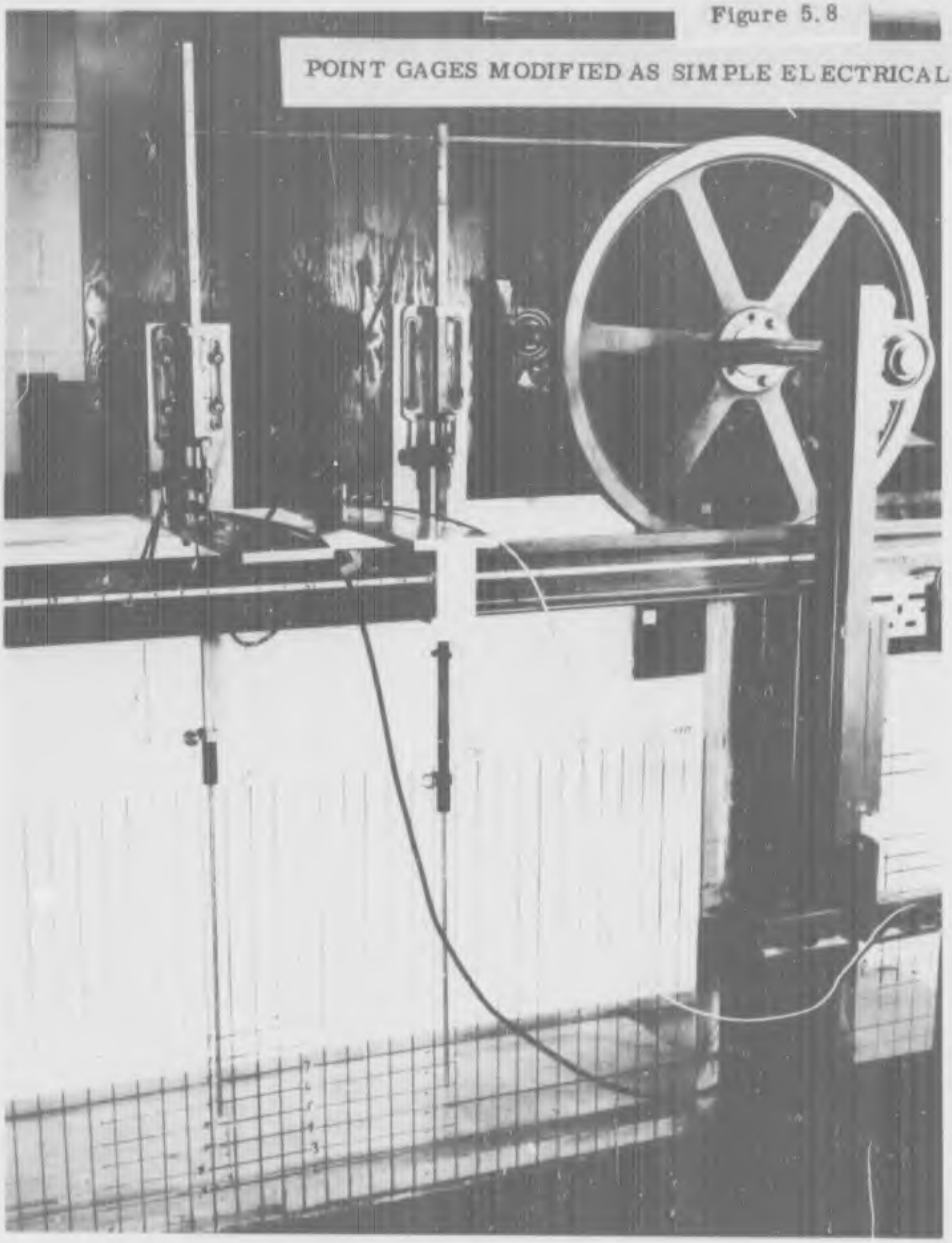

Figure 5.9

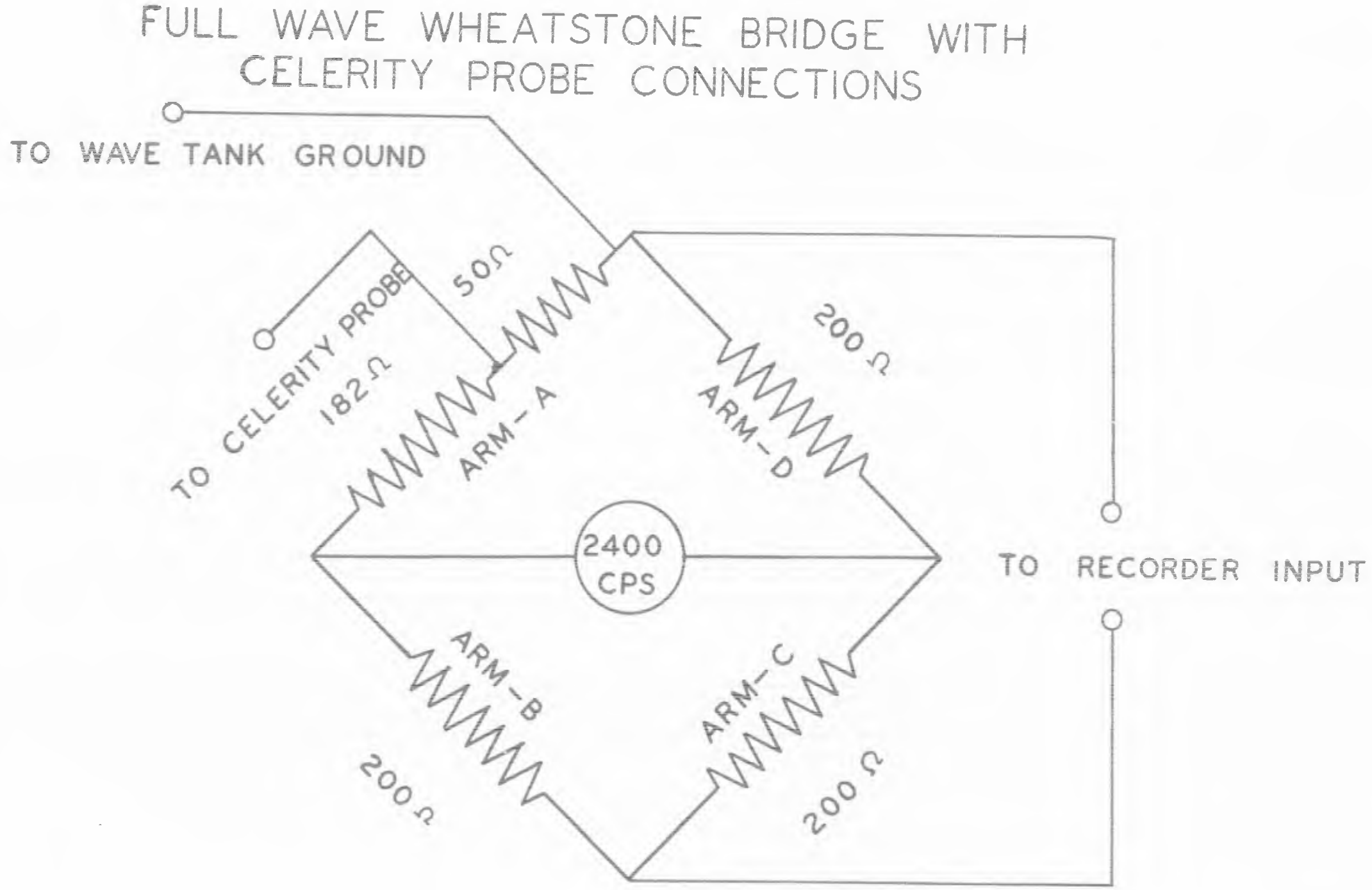
FULL WAVE WHEATSTONE BRIDGE WITH
CELERITY PROBE CONNECTIONS
TO WAVE TANK GROUND
TO CELERITY PROBE
182 Ω
50 Ω
200 Ω
ARM-A
ARM-D
2400
CPS
TO RECORDER INPUT
ARM-B
ARM-C
200 Ω
200 Ω

Figure 5.10a COMPARISON OF OSCILLOGRAPH RECORD WITH PHOTO

(Undulating surge at $y_2/y_1 = 1.37$)

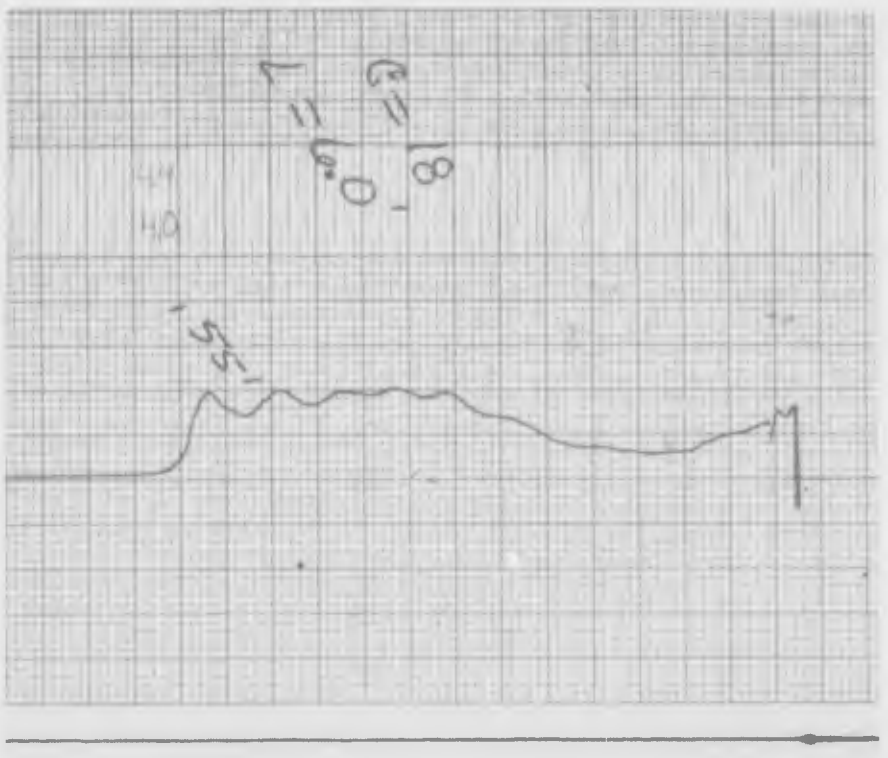

Figure 5.10b COMPARISON OF OSCILLOGRAPH RECORD WITH PHOTO
(Transition at $y_2 / y_1 = 1.57$)

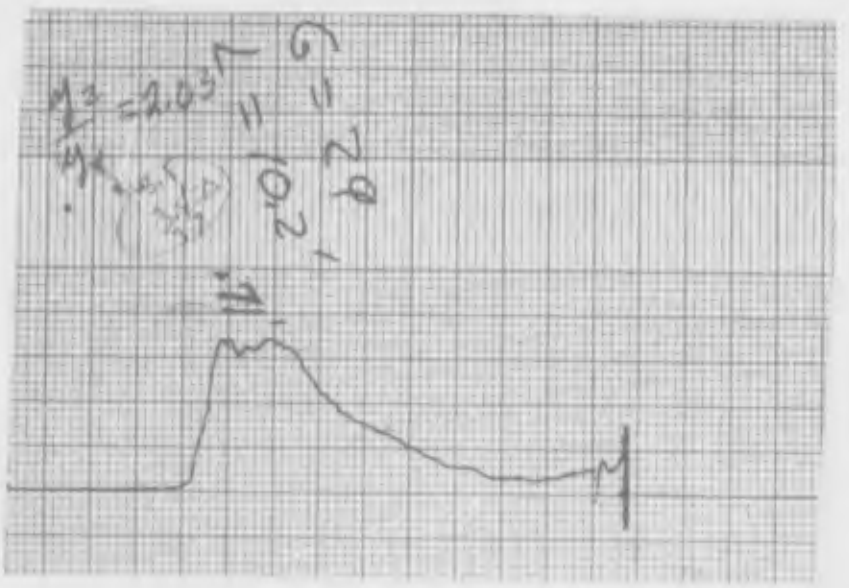

Figure 5.10c COMPARISON OF OSCILLOGRAPH RECORD WITH PHOTO
(Shock form at $y_2|y_1 = 2.03$)

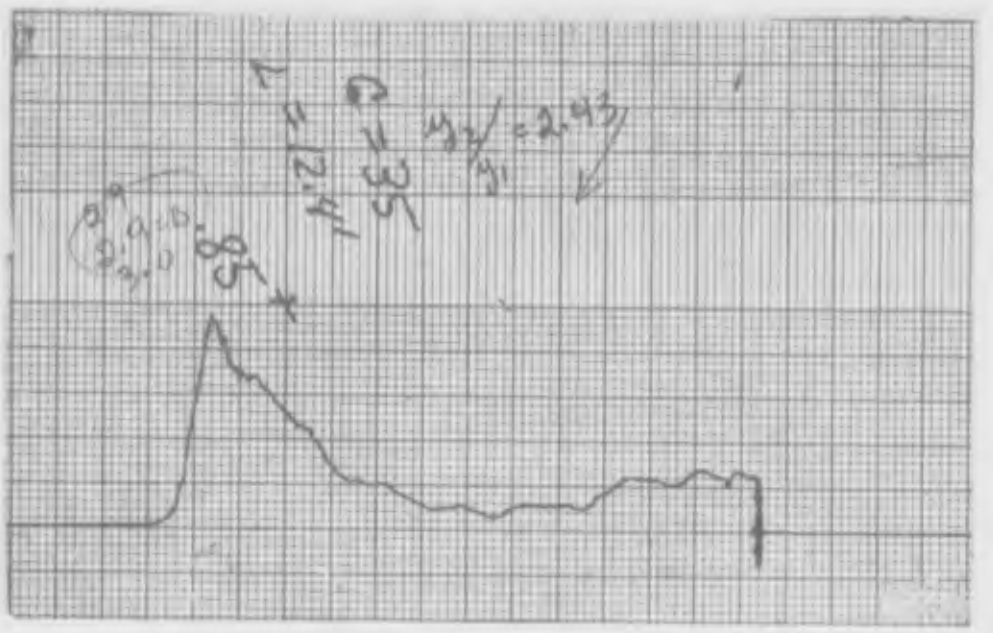

Figure 5.10d COMPARISON OF OSCILLOGRAPH RECORD WITH PHOTO
(Very turbulent shock form at $y_2 / y_1 = 2.43$)

Figure 6.1 INITIATION AND EARLY PHASES OF THE GRAVITY SHOCK WAVE

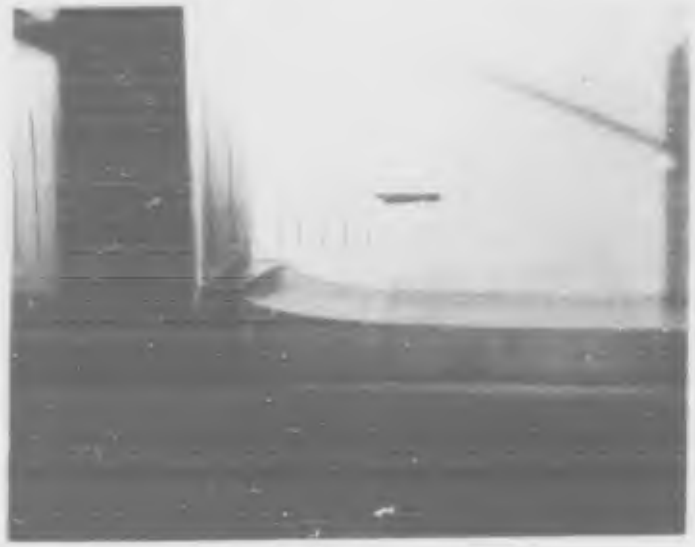

The first photo shows the initial stage just after piston begins acceleration from rest.

The second photo illustrates the beginning of the steep turbulent front and flat top.

The third photo illustrates the fully developed wave just before release from the piston.

Figure 6.2

DEFINITION SKETCH

(Based on a figure in Rouse, 1938)

V= PISTON VELOCITY (CONSIDERED EQUIVALENT TO U).

C= WAVE VELOCITY.

y_1= STILL-WATER DEPTH MEASURED FROM BOTTOM.

y_2= WAVE HEIGHT MEASURED FROM BOTTOM.

t_1, t_2= SUCCESIVE POSITIONS OF PISTON AT TIMES t_1, t_2.

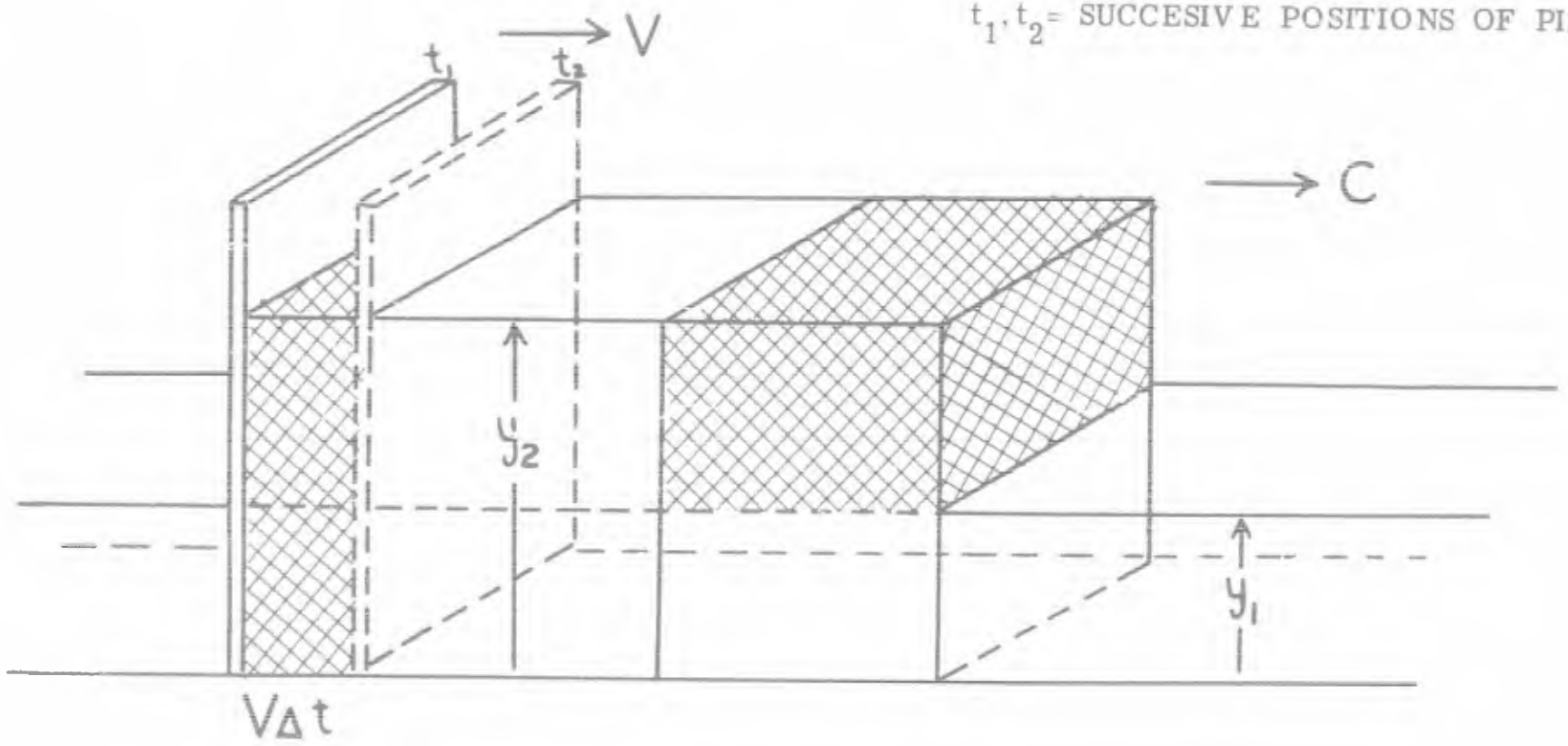

Figure 6.3 COMPARISON OF EXPERIMENTALLY DETERMINED V (equivalent to u) WITH THEORETICAL EXPECTATION OF V AS A FUNCTION OF y_2/y_1.

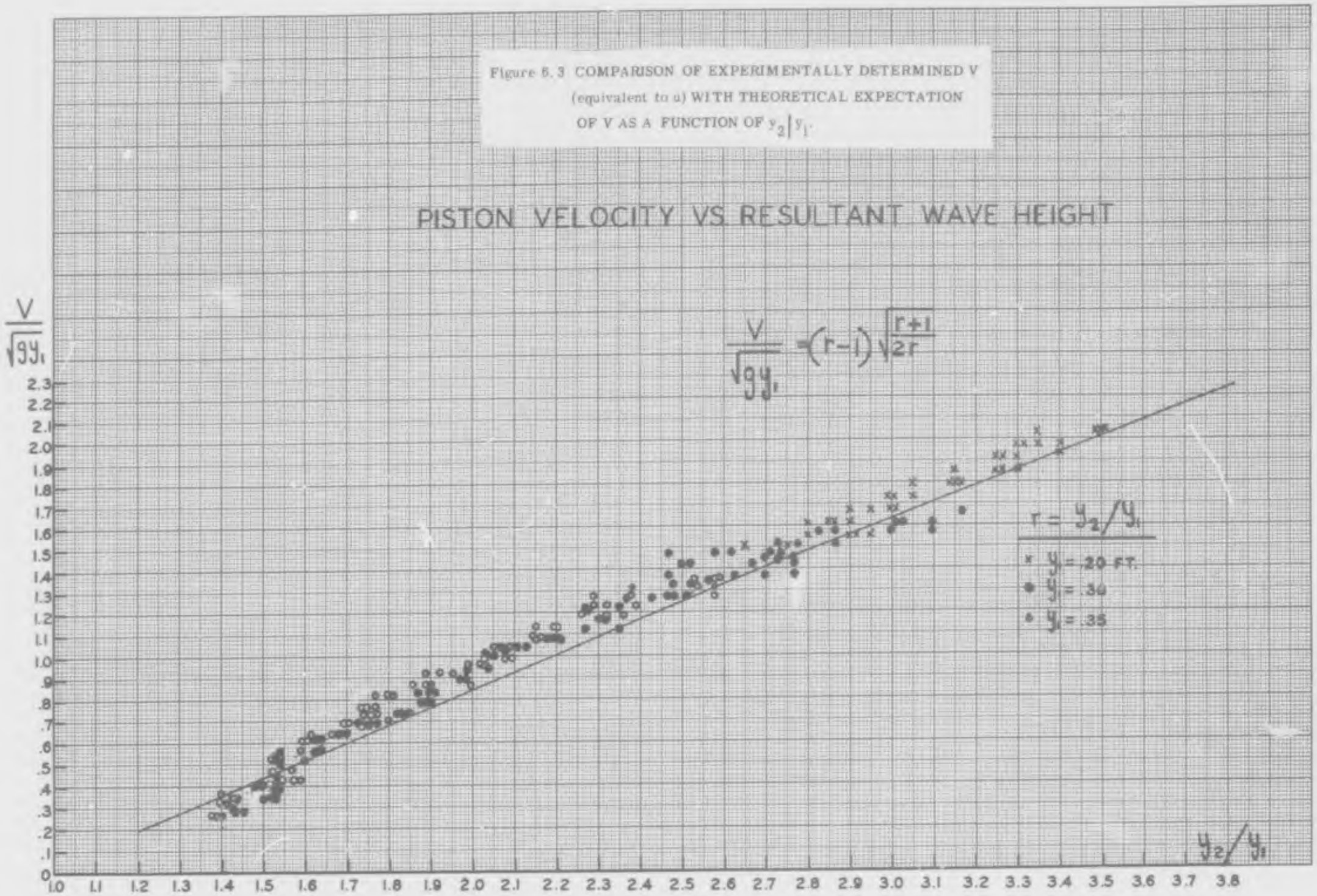

Figure 5.4

MOTION PICTURE PHOTOGRAPHY

AT 64 FRAMES PER SECOND

CELERITY MEASURED OVER A FOUR FRAME INTERVAL AT 1/16 SECOND.

EACH POINT IS THE AVERAGE FOR A RUN

$\frac{C}{\sqrt{gy_1}}$

$\frac{C}{\sqrt{gy_1}} = \left[\frac{1}{2}\, y_2/y_1 \left(y_2/y_1 + 1\right)\right]^{\frac{1}{2}}$

○ $\frac{y_1}{D}$ = 0.2 FT.

● $\frac{y_1}{D}$ = 0.3 FT.

y_2/y_1

Figure 6.5

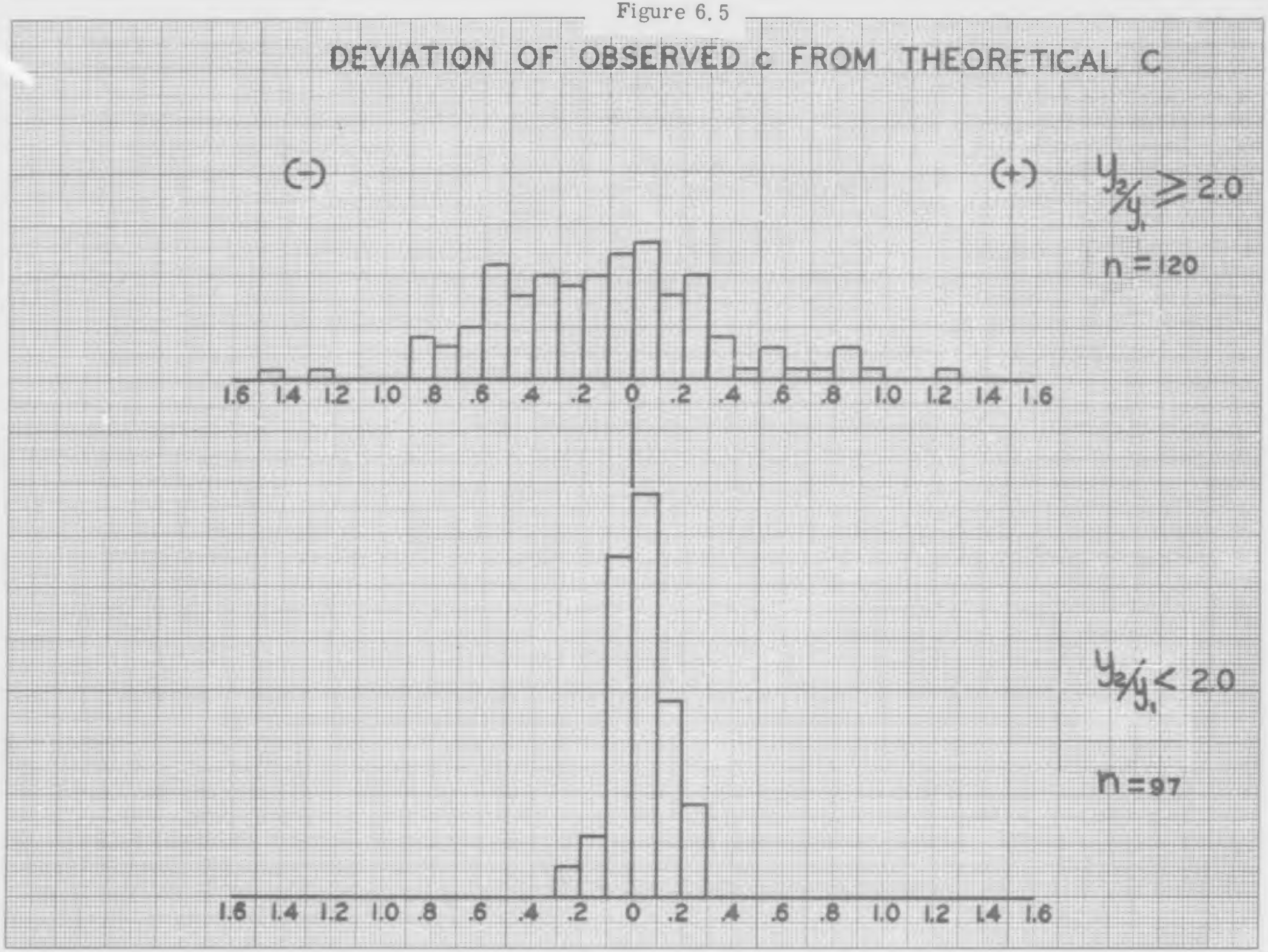
DEVIATION OF OBSERVED c FROM THEORETICAL C
(-)
(+)
$y_2/y_1 \geq 2.0$
n = 120
1.6 1.4 1.2 1.0 .8 .6 .4 .2 0 .2 .4 .6 .8 1.0 1.2 1.4 1.6
$y_2/y_1 < 2.0$
n = 97
1.6 1.4 1.2 1.0 .8 .6 .4 .2 0 .2 .4 .6 .8 1.0 1.2 1.4 1.6

DOCUMENT CONTROL DATA - R&D

(Security classification of title, body of abstract and indexing annotation must be entered when the overall report is classified)

1. ORIGINATING ACTIVITY *(Corporate author)*

University of Chicago

2a. REPORT SECURITY CLASSIFICATION

UNCLASSIFIED

2b. GROUP

3. REPORT TITLE

A single impulse-system for generating solitary, undulating surge, and gravity shock waves in the laboratory.

4. DESCRIPTIVE NOTES *(Type of report and inclusive dates)*

Technical Report

5. AUTHOR(S) *(Last name, first name, initial)*

Miller, Robert L. and White, Robert V.

6. REPORT DATE	7a. TOTAL NO. OF PAGES	7b. NO. OF REFS
June 1966	48	4

8a. CONTRACT OR GRANT NO.	9a. ORIGINATOR'S REPORT NUMBER(S)
Nonr 2121(26)	Technical Report No. 5
b. PROJECT NO.	
c. NR 388-074	9b. OTHER REPORT NO(S) *(Any other numbers that may be assigned this report)*
d.	

10. AVAILABILITY/LIMITATION NOTICES

11. SUPPLEMENTARY NOTES	12. SPONSORING MILITARY ACTIVITY
Support for equipment provided by NSF	Geography Branch Office of Naval Research Washington, D.C. 20360

13. ABSTRACT

A piston type system has been devised to create single-impulse wave for laboratory study. These include solitary waves, undulating surge and gravity shock waves. y_2/y_1 values as high as 4.0 have been obtained, which for a still water depth (y_1) of 0.4' would result in a y_2/y_1 ratio of 1.6'. Details of design and construction are given. Calibration and comparison of observed vs. expected wave properties are discussed. Included in these sections are application of strobe flash and high speed motion picture techniques.

DD FORM 1 JAN 64 1473

023558

UNCLASSIFIED
Security Classification